Diatom Frustules as Substrates for Photocatalysts

N. Day, J. Olsen, V. Dereviankin, J. Thiebes, B. Beyers, A. Polliack

Diatomix, Beaverton, OR, USA, nick@diatomixcorp.com

ABSTRACT

Heterogeneous catalyst supports are an active area of research especially for nanomaterial catalysts. We studied the effects of three types of diatomite as the support for titanium dioxide photocatalysts. Diatomaceous earth samples were obtained and characterized via scanning electron microscopy, energy dispersive x-ray spectroscopy and surface area. Then each support was coated with photocatalytic titanium dioxide using the identical synthesis procedure. Photocatalytic rates were measured using a photo-ionization detector to measure the complete destruction of acetone and its by-products. The rate of photocatalysis is compared to the surface areas and other determined characteristics of the diatomaceous earth samples. The results suggest that intact diatom supports increase incident photons upon the photocatalysts giving higher rates of photocatalytic destruction.

Keywords: catalyst support, photocatalysis, diatomaceous earth, titanium dioxide, volatile organic compounds

1 INTRODUCTION

Many industrial syntheses are now made possible by the optimization of heterogeneous catalysts.[1-3] Heterogeneous catalysts have been improved through the use of high surface area nanomaterials, both nanoparticle catalysts and nanopatterned supports.[1] Nanomaterial catalysts allow excellent reaction rates but are difficult to separate from reactants.[1] As such, inert catalyst supports are used and have been optimized to provide higher surface areas, reaction specificity, thermal resistance, higher catalyst recovery and other properties.[1]

Heterogenous photocatalysts are less used in industry yet light is an ideal reagent for environmental friendly reactions.[4] The ability to use photo-induced excited states to drive reactions over the activation barrier can lead to cost savings and more environmentally friendly processes.

Supports for heterogeneous photocatalysis will need special considerations for optimal rates of reaction. These include optical transparency for the wavelengths of light which activate the catalyst and no adverse effects on excited state lifetimes. In addition the best substrates for heterogeneous photocatalysts can be optimized to increase excited state lifetimes and assist in the capture of light. Little literature can be found addressing the ability of using a photocatalyst substrate to help capture the light energy. Many publications address a photosensitizer to drive catalysis but this is fundamentally different than a substrate that can redirect the light to the photocatalyst.[5]

Herein we report our findings using diatom frustules as the substrate for titanium dioxide photocatalysts. Other groups have also used diatomaceous earth (DE) as a substrate for titanium dioxide photocatalysts.[6-10] Diatom frustules have previously been shown to trap light with 380 to 550 nm wavelengths by 1.5 to 1.7x.[11,12] This interesting function has been suggested for improving thin-film solar cells but has not been explored for photocatalysts. Titanium dioxide was chosen for use because of its activity in the proper ranges of trapped light and its availability.[13] In addition, we have developed proprietary synthesis methods to deposit the titanium dioxide preferentially in the pores of the diatom frustule shells. This deposition primarily on the pores allows us to determine if the light trapping effects can be utilized for increased incident photon absorption by the photocatlyst.

2 EXPERIMENTAL

2.1 Materials and Equipment

Three distinct types of DE samples were used. All three samples are amorphous materials and contain different primary genera of diatoms. The first sample referred to as B1 is primarily an intact barrel-shaped diatom of genus *Aulacoseira*. The second DE is refered to as C1 and is also primarily intact but disc-shaped of genus *Stephanodiscus*. The third DE, referred to as D1 is a mixture of diatoms including *Stephanodiscus*, *Melosira* and *Cyclotella* but most of the diatoms are broken and few distinct shapes can be seen under SEM analysis. Figure 1 shows a zoomed out view of the DE samples with an example of each.

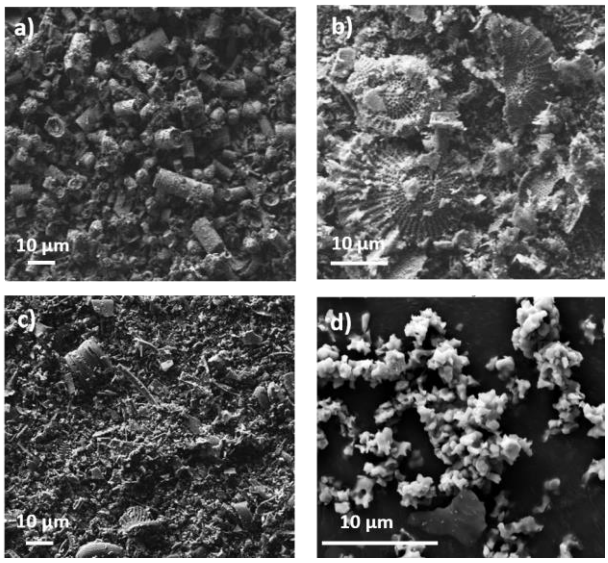

Figure 1: SEM images of all DE starting samples as well as synthesized TiO_2, taken as an overview to show genus variety, intactness of each DE sample and size, B1 (a), C1 (b), D1 (c), and TiO_2 (d).

Titanium oxysulfate ($TiOSO_4 \bullet xH_2O$) was obtained from Sigma-Aldrich, acetone was obtained from Alfa Aesar while DE was from Imerys and Dicalite.

2.2 Synthesis

Preparation of the final products was performed using a proprietary hydrothermal method. All products were synthesized identically and annealed in a programmable furnace with a final temperature of 400 °C.

2.3 Testing

The concentration of titanium dioxide on each sample was determined by colorimetry using concentrated H_2SO_4 to redissolve the titanium dioxide and then hydrogen peroxide to produce peroxotitanic acid. First 5 mL of concentrated H_2SO_4 was heated in a test tube with a stir bar to 175 °C. Then 0.1 g of the DE coated TiO_2 sample was added and allowed to dissolve for 30 minutes. Then the reaction was cooled, quenched and filtered through a 0.45 µm syringe filter. Finally 30% hydrogen peroxide was added. Peroxotitanic acid concentration was determined using Beer's law and a spectrophotometer at 400 nm.

The percent of titanium dioxide in the pore was determined by energy dispersive x-ray spectroscopy (EDS) analysis for titanium on the diatoms and subsequent analysis using image-J software[14] for the number of pixels located inside the pore compared to those on the rest of the diatom frustule. All images were analyzed identically.

The products were tested for photocatalytic activity by sealing samples of a fixed mass distributed across a fixed area substrate that was placed inside a test chamber. The mass was fixed to have the equivalent amount of total TiO_2 in the testing chamber. The products were exposed to a fixed concentration of acetone, irradiated with 365 nm LED light, and concentration of acetone and degradation by-products was monitored over time using a photoionization detector (PID). The metric for photocatalytic activity was chosen to be the rate of degradation of acetone, measured between 30% and 70% total degradation and was compared to hydrothermally synthesized TiO_2 rate.

Surface area of the materials was studied using NOVA2200e gas sorption analyzer. Surface area analysis was performed using 6 point BET method, while DFT method was used for pore size and volume assessment.

3 RESULTS

The synthesis method has repeatedly proven to deposit titanium dioxide in the pores of the diatom frustules. Figure 2 shows EDS mapping of titanium for multiple diatom/TiO_2 samples for different diatom species, which is indicative of the titanium dioxide photocatalyst. Titanium is preferentially located in the pores of the diatom frustules. These pores act as the light guides into and out of the diatom frustules and should be the primary place where light is concentrated. As such the deposition of the photocatalyst in these pores is a primary concern for determining if the light concentration effects can be utilized. The barrel diatom, B1, was analyzed to have a concentration of around 70% of titanium concentrated in the pore areas. The disc diatom, C1, was analyzed to have around 65% of the titanium concentrated in the pores.

Surface area measurements of the materials were carried out using BET to characterize the differences between the DE and DE/TiO_2 samples. All DE samples had nominally the same average particle size, around 10 µm. In addition, two DEs were chosen to have similar surface areas, B1 at 53 ± 2 m^2/g and D1 at 50 m^2/g. B1 had mostly intact diatoms while the other, D1, contained a majority of broken structures. C1 has a significantly higher surface area at 133 ± m^2/g and was used to establish that higher surface areas and by correlation, adsorption rates, were not the cause of apparent increased photocatalysis.

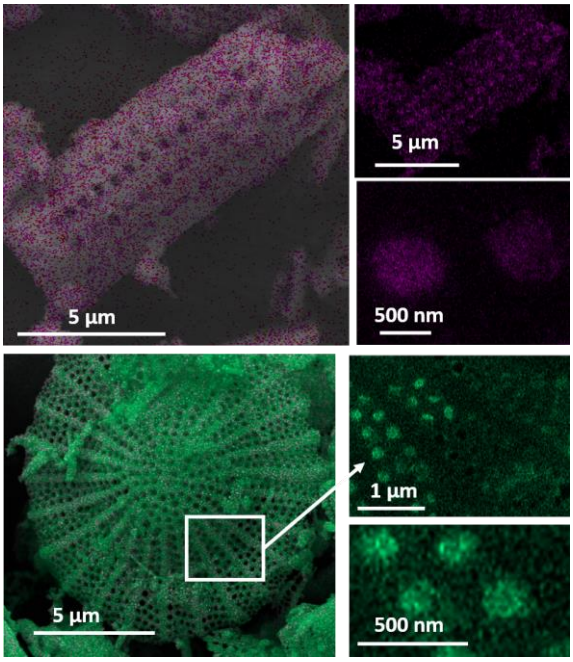

Figure 2: Left column: SEM/EDS of Diatom frustule coated via Diatomix proprietary method to deposit TiO_2 primarily in the pores. Right column: EDX map of the same diatom frustules to showing only the titanium mapping (top: B1 diatom showing Ti as purple. Bottom: C1 diatom showing Ti in green).

The photocatalytic results for the TiO_2 containing materials are shown in Figure 3 illustrating the relative destruction rates of VOCs by each product. The TiO_2 control had the slowest rate of photocatalytic degradation of acetone and its by-products' (VOCs) when compared to DE/TiO_2 samples, 0.08 %/sec. B1 and C1 samples, both containg mostly intact diatoms, showed the fastest rates of removal of VOCs, at 0.12 and 0.13 %/sec. Sample D1 containing mostly broken diatom frustules showed a rate similar to that observed for titanium dioxide, at 0.09 %/sec, and much slower than that of samples B1 and C1. It should be stated that all samples were tested with an identical starting concentration around 91 ± 3 units. Each unit corresponds to approximately 5 ppb response to isobutylene on the PID. The results suggest that intact diatoms are an important contributor to the increase in reaction rates and is more significant than the increase in surface area.

Table 1: Summarized characteristics of DE and DE/TiO2 samples.

Sample	Average Particle Size (µm)	Surface Area (m^2/g)	TiO_2 Content (%)	TiO_2 in Pore (%)
B1-Base	10 ± 3	53 ± 2	--	--
B1	10 ± 3	74 ± 2	19 ± 1	73
C1-Base	10 ± 3	133 ± 2	--	--
C1	10 ± 3	218 ± 2	21 ± 3	65
D1-Base	10 ± 3	50 ± 2	--	--
D1	10 ± 3	*75 ± 2*	20 ± 1	--
TiO_2	1 ± 0.5	45 ± 2	100	--

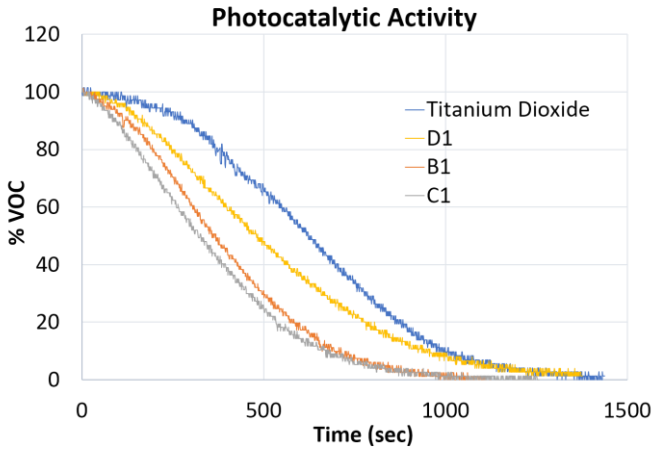

Figure 3: Photocatalytic degradation curves of various synthesis products compared against that of TiO_2. The legend is in the same order from top to bottom as the curves.

The increased surface area of sample C1 does not appear to have contributed to an increase in the rate of photocatalysis. In addition, D1 having an identical surface area to sample B1 did not show similar reaction rates. With sample D1's rate being only slightly faster than the TiO_2 control, and significantly slower than either of the intact diatom samples, B1 and C1, we can not attribute the faster rate of photocatalysis to the surface area of the DE base. Surface area should correlate with the quantity of material which becomes adsorbed, and this suggests that the increase in the rate of photocatalysis is not only due to higher adsorption of VOCs.

Table 2: The average rate of photocatalytic degradation of acetone by the various samples, as measured between 30% and 70% of total degradation curves shown if Figure 3.

Sample	Average VOC degradation rate (%/sec)	Relative to TiO_2
B1	0.13	1.6
C1	0.12	1.5
D1	0.09	1.1
TiO_2	0.08	1.0

4 CONCLUSION

The DE/TiO_2 samples with largely intact diatoms clearly out-performed the sample which contained a majority of broken diatom frustules. This is a unique finding which points towards the ability of intact diatoms to hold a distinct advantage for their use as supports for photocatalysts. In addition, of the intact DE genera used the increased surface area of C1, as compared to that of B1, was not observed to be responsible for the increase in the rate of destruction of acetone. This suggests that surface adsorption is not the mechanism causing the increase in the rate of loss of acetone. More testing is underway to further understand adsorption and surface area effects on degradation rates.

Considering the results for the degradation rates of the identically produced TiO_2 samples but supported by different DE substrates and the lack of a correlation between the increased rates and surface area, we believe the increase in photocatalysis is due to the light trapping effects of diatoms. This light trapping effect as reported in the literature correlates closely with the increased rate of photocatalysis seen, around 1.5 times.[11] As such, intact diatoms may offer a unique advantage as supports for photocatalysts. This light trapping advantage, along with high surface area, inert reactivity, and optical transparency make diatoms an excellent choice for photocatalyst supports. Diatoms may offer the potential to use significantly less expensive photocatalysts in order to achieve similar or higher reaction rates.

More studies with other photocatalysts, reactants and diatom substrates are ongoing to elucidate the causes of the increased rates of photocatalysis.

5 ACKNOWLEDGMENTS

We would like to thank the Oregon Nanomaterials and Manufacturing Institute (ONAMI) and the National Science Foundation as well as our other supporters including, Lectrix, Reference Capital and the Willamette Angel group.

REFERENCES

(1) Munnik, P.; de Jongh, P. E.; de Jong, K. P. Recent Developments in the Synthesis of Supported Catalysts. *Chem. Rev.* **2015**, *115* (14), 6687–6718.

(2) Liu, Y.; Zhao, G.; Wang, D.; Li, Y. Heterogeneous Catalysis for Green Chemistry Based on Nanocrystals. *Natl. Sci. Rev.* **2015**, *2* (2), 150–166.

(3) Busca, G. *Heterogeneous Catalytic Materials: Solid State Chemistry, Surface Chemistry and Catalytic Behaviour*; Newnes, 2014.

(4) Yoon, T. P.; Ischay, M. A.; Du, J. Visible Light Photocatalysis as a Greener Approach to Photochemical Synthesis. *Nat. Chem.* **2010**, *2* (7), 527–532.

(5) Andreiadis Eugen S.; Chavarot-Kerlidou Murielle; Fontecave Marc; Artero Vincent. Artificial Photosynthesis: From Molecular Catalysts for Light-driven Water Splitting to Photoelectrochemical Cells. *Photochem. Photobiol.* **2011**, *87* (5), 946–964.

(6) Chen, Y.; Liu, K. Preparation of Granulated N-Doped TiO_2/Diatomite Composite and Its Applications of Visible Light Degradation and Disinfection. *Powder Technol.* **2016**, *303*, 176–191.

(7) Mao, L.; Liu, J.; Zhu, S.; Zhang, D.; Chen, Z.; Chen, C. Sonochemical Fabrication of Mesoporous TiO_2 inside Diatom Frustules for Photocatalyst. *Ultrason. Sonochem.* **2013**, *21*.

(8) Padmanabhan, S. K.; Pal, S.; Ul Haq, E.; Licciulli, A. Nanocrystalline TiO2–diatomite Composite Catalysts: Effect of Crystallization on the Photocatalytic Degradation of Rhodamine B. *Appl. Catal. Gen.* **2014**, *485* (Supplement C), 157–162.

(9) Zhang, G.; Sun, Z.; Duan, Y.; Ma, R.; Zheng, S. Synthesis of Nano-TiO_2/Diatomite Composite and Its Photocatalytic Degradation of Gaseous Formaldehyde. *Appl. Surf. Sci.* **2017**, *412*, 105–112.

(10) Wu, Z.; Zhu, Z.; Hao, X.; Zhou, W.; Han, J.; Tang, X.; Yao, S.; Zhang, X. Enhanced Oxidation of Naphthalene Using Plasma Activation of TiO_2/Diatomite Catalyst. *J. Hazard. Mater.* **2018**, *347*, 48–57.

(11) Chen, X.; Wang, C.; Baker, E.; Sun, C. Numerical and Experimental Investigation of Light Trapping Effect of Nanostructured Diatom Frustules. *Sci. Rep.* **2015**, *5*, 11977.

(12) Fuhrmann, T.; Landwehr, S.; Rharbi-Kucki, M. E.; Sumper, M. Diatoms as Living Photonic Crystals. *Appl. Phys. B* **2004**, *78* (3–4), 257–260.

(13) Jeffryes, C.; Campbell, J.; Li, H.; Jiao, J.; Rorrer, G. The Potential of Diatom Nanobiotechnology for Applications in Solar Cells, Batteries, and Electroluminescent Devices. *Energy Environ. Sci.* **2011**, *4* (10), 3930–3941.

(14) Schneider, C. A. *NIH Image to ImageJ: 25 Years of Image Analysis*; 2012; Vol. 9(7).